

# SIMULATION OF A FLAT CAPILLARY HEAT PIPE USING AN INTERFACE TRACKING METHOD

**Humberto Araujo Machado**

Universidade do Vale do Paraíba – UNIVAP, Instituto de Pesquisa e Desenvolvimento – IP&D  
Av. Shishima Hifume, 2911, Urbanova, 12244-000, São José dos Campos, SP, Brazil  
[machado@univap.br](mailto:machado@univap.br)

**Abstract.** In capillary and micro heat pipes the internal porous media is replaced by a capillary groove, yielding a meniscus formed by the liquid phase. The meniscus height varies along the groove length, from the condenser section to the evaporator section, and the difference between the pressures in each extremity is responsible for pumping the liquid. Such devices have been employed in electronic cooling, due its small dimensions. This system provides excellent thermal control, assuring uniform temperature distribution. In previous works related to capillary heat pipe simulation, empirical or simple 1-D models have been used, but not taking into account the complete unsteady phenomena. In this work, the physical model and the 2-D unsteady simulation of a flat capillary heat pipe is presented. The phase change problem of a heated liquid meniscus in a groove is simulated via an interface tracking method, which is an hybrid Lagrangean-Eulerian method for moving boundary simulation. A variation of the one-dimensional Stephan problem is used to validate the numerical code.

**Key words:** Capillary meniscus, Interface tracking, Phase change, Moving boundary

## 1. Introduction

Phase change processes through capillary grooves are commonly incorporated in design of heat exchangers, increasing the interfacial areas among liquid-vapor phases for evaporation and vapor-liquid phases for condensation. These grooves allow the liquid phase to coalesce and move from the condensation region for the evaporator, promoting the reduction of thickness of the liquid film. Recently, the use of such systems in microscale devices for cooling of electronic equipment has deserved attention, due its high heat transfer rates and excellent thermal control, improving the uniformity of temperature distribution, specially when employed as micro heat pipes, that are built straight over the chips structure. Mini and micro heat pipes have been employed in high performance computers, laptops and workstations, satellites and space probes, fine surgery instruments, etc.

The development of this kind of heat pipe has been done using empirical methods or simplified models. Most of the experimental works deal with a specific aspect of micro heat pipes, such as a particular shape or phenomenon involved in the pipe operation, or accuracy of any theoretical approximation used in the model. In these cases, some information is available about thermocapillary effects in a heated meniscus (Prat *et al*, 1998) or about the influence of geometry in the heat exchange process (Ravigururajan, 1998). In all experiments, several difficulties were found in reproducing the realistic dimensions and conditions of operation of a feasible M.H.P (Faghri, 1995). Duncan and Peterson (1994) summarized the conclusions and limitations of each model available in a opened literature review. Krushtalev and Faghri (1994) have shown an one-dimensional model to predict the maximum heat exchange capacity and thermal resistance of a polygonal M.H.P, which was developed from some approximations based in empirical observations.

Ma & Peterson (1998) investigated the minimum meniscus radius and the heat exchange limit in M.H.P through the conservation laws for momentum and Laplace-Young equation, providing analytical expressions for parameters of interest. Ha & Peterson (1998) have been developed a model where the differential expression is similar to Bernoulli's equation. An approximate analytical solution for the axial variation of meniscus curvature is presented. Peterson & Ma (1999) developed a more detailed model for a M.H.P through a 3<sup>th</sup> order ordinary differential equation, that is able to estimate the heat transport capacity and the temperature gradients along longitudinal coordinate, as a function of heat flux. However, all these works are 1-D models, just applicable to steady state processes.

The present work is an extension of the work presented by Machado & Miranda (2001), where a mathematical model and a computational algorithm for simulation of the unsteady heat transfer process in an opened square cavity, representing a flat capillary heat pipe, was proposed. In this work, a closed cavity is used to simulate the actual behavior of a capillary heat pipe. The phase change problem is solved via the interface tracking method proposed by Unverdi and Trygvason (1992), that is an hybrid Lagrangean-Eulerian method for moving boundaries, and has been employed to simulate fusion/solidification of crystals and metal alloys and bubble formation in nucleate boiling. Preliminary results show the behavior of the computer code for a simple case. The model proposed here may be easily extended to 3-D problems with irregular geometries.

## 2. Physical problem and mathematical model

Consider a square cavity, filled with a pure Newtonian fluid with constant properties and isochoric behavior, showed in Fig. (1). Thermodynamic equilibrium is assumed in both phases, liquid and vapor, inside. The lateral and superior sides are thermally insulated. Thermal and viscous effects in transversal direction are neglected.

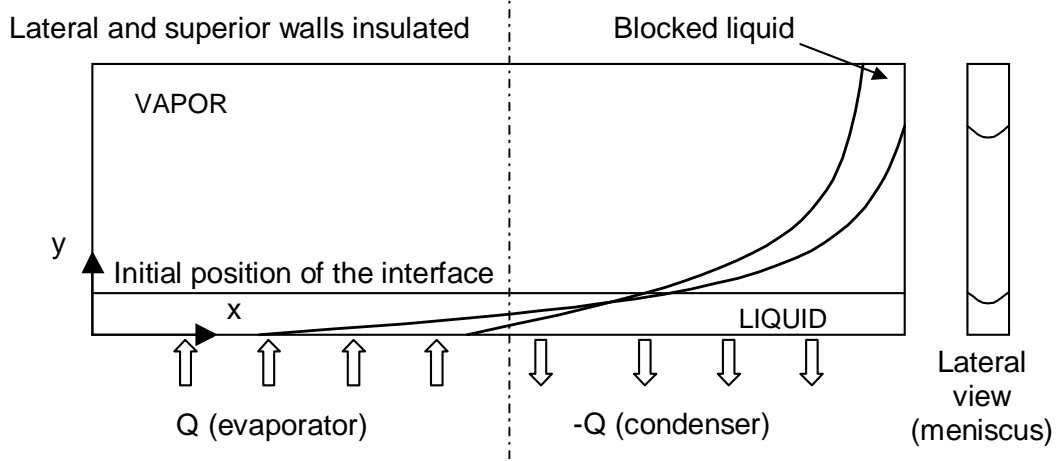


Figure 2. Schematic of the geometry and physical process.

The set of equations in dimensionless form used to represent the simple physical problem is written according to the interface tracking method, as proposed by Juric (1996). Terms in bold are vector quantities.

Continuity equation:

$$\frac{\partial \rho}{\partial t} + \nabla \cdot \mathbf{w} = 0 \quad (1)$$

that is better represented by:

$$\nabla \cdot \mathbf{w} = M \quad (2)$$

$$M = \int_A m \delta(\mathbf{x} - \mathbf{x}_f) dA \quad (3)$$

$$m = \left( \frac{\rho_v}{\rho_l} \right) \mathbf{V} \cdot \mathbf{n} \quad (4)$$

where  $\mathbf{w} = \rho \mathbf{u}$  (mass flux),  $\mathbf{V}$  is the interface velocity,  $\mathbf{n}$  is the interface normal vector,  $m$  is the mass flux through the interface per unit of area and  $\delta(\mathbf{x} - \mathbf{x}_f)$  is a 3-D delta function, that is non-zero only at the interface. Subscripts  $l$  and  $v$  refers to liquid and vapor phases, respectively. Tangential effects are neglected as the fluid properties are assumed constant and uniform in each phase. Therefore, the interface velocity is supposed not having a tangential component. Such assumptions should be verified carefully, in a more detailed model.

Conservation of momentum:

$$\frac{\partial(\rho \mathbf{u})}{\partial t} + \nabla \cdot (\rho \mathbf{u} \mathbf{u}) = -\nabla P + \frac{1}{Re} \nabla \cdot \mu (\nabla \mathbf{u} + \nabla \mathbf{u}^T) + \mathbf{F} \quad (5)$$

where  $P$  is the pressure and  $\mathbf{F}$  is a source term that takes into account the interfacial surface forces:

$$\mathbf{F} = \int_A \mathbf{f} \delta(\mathbf{x} - \mathbf{x}_f) dA \quad (6)$$

where  $\mathbf{x}_f$  is the interface position vector,  $\mathbf{f}$  is the interface pressure due to the surface tension:  $\mathbf{f} = \kappa \mathbf{n} / We$ , and  $\kappa$  is twice the mean curvature of the interface.

Conservation of energy:

$$\frac{\partial(\rho c T)}{\partial t} + \nabla \cdot (\rho c T \mathbf{u}) = \frac{1}{Pe} \nabla \cdot K \nabla T + Q \quad (7)$$

where  $c$  is the specific heat at constant pressure,  $K$  is the thermal conductivity and  $Q$  is a source term that takes into account the absorption or liberation of latent heat during phase change:

$$Q = \int_A q \delta(\mathbf{x} - \mathbf{x}_f) dA \quad (8)$$

$q$  is the source term of energy per unit of surface of the interface:

$$q = \frac{\rho_l L}{\rho_v L_0} (\rho \mathbf{V} - \mathbf{w}) \cdot \mathbf{n} \quad (9)$$

where  $L_0$  is the latent heat of phase change and  $L$  is its corrected form, taking into account different specific heats for each phase:

$$L = L_0 + (c_l - c_v) T_v \quad (10)$$

The equations above, with the source terms included, satisfy the jump conditions automatically, assuming a thickness interface.

Although specific volumes are different in the phases, the flow is assumed to be incompressible, and both densities are considered constant. The total volume occupied for each phase remains constant during the heating. Therefore, the rates of condensation and evaporation must be the same, in order to satisfy the mass conservation within the cavity. During the transient process of heat transfer, the reference pressure inside the cavity rises and yields a correspondent increase of the local saturation temperature in every interface point, until the flow reaches steady state.

The interface is supposed to be at thermal but not thermodynamic equilibrium (which supposes no temperature jump at the interface). This hypothesis added to the Clausius-Clapeyron relation applied to a curved surface, but neglecting the kinetic mobility effects yields the temperature condition at the interface as a function of the reference pressure:

$$T_f - T_{SAT} - \sigma \kappa + We \cdot T_{SAT} \left( 1 - \frac{\rho_l}{\rho_v} \right) (P_f - P_\infty) + \frac{\rho_v}{\rho_l} \left( \frac{c_v}{c_l} - 1 \right) (T_f - T_{SAT})^2 + \vartheta (\rho \mathbf{V} - \mathbf{w}) \cdot \mathbf{n} = 0 \quad (11)$$

where  $T_f$  is the local interface temperature,  $T_{SAT}$  is the local saturation temperature (from the equation of state),  $P_f$  is the local interface pressure,  $P_\infty$  is the reference pressure within the cavity,  $\sigma = c_l T_o \gamma / \rho_v L_0^2 y_o$ .  $T_o$  is the reference temperature,  $y_o$  is the reference length and  $\gamma$  is the surface tension. Last term includes the non-equilibrium effects in the molecular kinetics:  $\vartheta = \rho_l c_l U_o / \rho_v L_0 \phi$ , where  $\phi$  is the molecular kinetics coefficient. Small values of  $\phi$  suppress the growth of protrusions in the interface.

The non-dimensional numbers resulting from the mathematical model are: Reynolds number,  $Re = \rho_l U_o l / \mu_l$ , Peclet number,  $Pe = Re \cdot Pr$ , Weber number,  $We = \rho_l U_o^2 l / \gamma$  and Froude number,  $Fr = U_o^2 / G \cdot y_o$  ( $G$  is the local acceleration of gravity).

### 3. Method of solution

The moving boundary problem was solved by the Interface Tracking Method, introduced by Unverdi & Trygvason (1992), and employed by Juric (1996) in the solution of phase change problems. In this method, a fixed uniform Eulerian grid is generated, where the conservation laws are applied over the complete domain. The interface acts as a Lagrangean referential, where a moving grid is applied. The instantaneous placement of the interface occurs through the constant remeshing of the moving grid, and each phase is characterized by the Indicator Function, represented by  $I(\mathbf{x}, t)$ , which identifies the properties of vapor and liquid phases.

The interface is represented as a parametric curve,  $\mathbf{R}(u)$ , where the normal and tangent vectors and curvature are extracted from. The interface points are interpolated by a Lagrange polynomial, which allows to obtain the geometric parameters and remeshes the curve, keeping the distance  $d$  between curve points within the interval  $0.9 < d/h < 1.1$ , where  $h$  is the distance among the fixed grid points, as shown in Fig. (2).

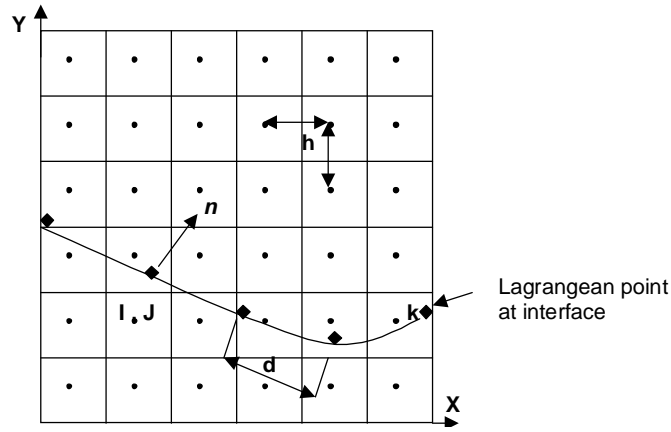


Figure 2. Eulerian and Lagrange meshes.

The Indicator Function varies from 1 (vapor) to 0 (liquid), and is numerically constructed using the interface curve to determine a source term  $\mathbf{G}(\mathbf{x})$ . The jump across the interface is distributed over the fixed grid points, yielding a gradient field in the mesh:

$$\mathbf{G}(\mathbf{x}) = \nabla I = \int_A \mathbf{n} \delta(\mathbf{x} - \mathbf{x}_f) dA \quad (12)$$

which should be zero, except over the interface, as represented by the Dirac Delta Function. However, such representation is not convenient for a discrete number of points. The Distribution Function is used to represent the interface jump. Such Function is a curve similar to a Gaussian one, as shown in Fig (3), and its value depends on the distance  $|\mathbf{x}_{ij} - \mathbf{x}_k|$  among the Lagrangean and Eulerian points:

$$D_{ij}(\mathbf{x}_k) = \frac{f[(x_k - x_i)/h].f[(y_k - y_j)/h]}{h^2} \quad (13)$$

where  $D_{ij}$  is the Distribution Function for a point  $k$  in the Lagrangian mesh in relation to a Eulerian point. One should note that increasing  $h$ , the interface becomes thicker. The function  $f$  is the probability distribution, related to the distance  $h$  as:

$$f(x) = \begin{cases} f_1(x) & \text{se } |x| \leq 1 \\ 1/2 - f_1(2 - |x|) & \text{se } 1 < |x| < 2 \\ 0 & \text{se } |x| \geq 2 \end{cases} \quad (14.a)$$

$$f_1(x) = \frac{3 - 2|x| + \sqrt{1 + 4|x| - 4x^2}}{8} \quad (14.b)$$

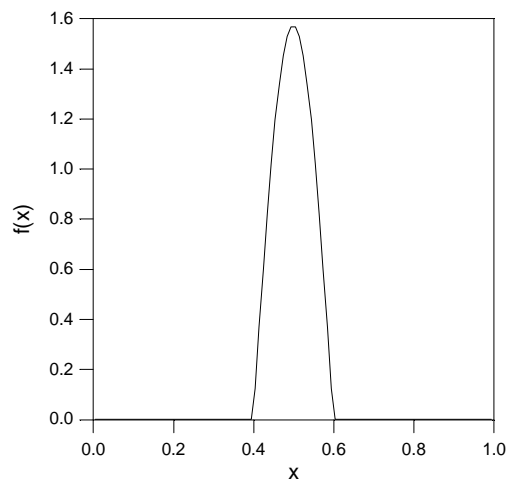


Figure 3. Probabilistic distribution profile -  $f(x)$ .

The divergence of the gradient field is found by numerical derivation of Poisson's equation:

$$\nabla^2 I = \nabla \cdot \mathbf{G} \quad (15)$$

Despite of being considered constants in each phase, the properties inside the domain must be treated as variable in the formulation. A generic property  $\phi$  ( $\rho$ ,  $\mu$ ,  $c$  ou  $K$ ) is expressed as:

$$\phi(\mathbf{x}) = \phi_l + (\phi_v - \phi_l) I(\mathbf{x}, t) \quad (16)$$

The coupling between the moving mesh and the fixed grid is done at each time step, through the Distribution Function, that represents the source terms in the balance equations and interpolate the fields with infinitesimal discontinuities into a finite thick region at the interface. The momentum equation at the interface surface becomes:

$$\frac{\partial I}{\partial t} = -\mathbf{V} \cdot \nabla I \quad (17)$$

The initial interface shape is first specified and then the Indicator Function is constructed. The property and temperature fields are determined. The iterative process targets the reference pressure and its correspondent interface velocity at each time step. The steps to be followed are:

1. Using the current value of  $\mathbf{V}$ , the interface points are transported to a new position, calculated explicitly through the equation  $\mathbf{V}^n = (d\mathbf{x}_f/dt) \cdot \mathbf{n}$ ;
2. Density and specific heat are calculated at the new interface position;
3. Surface tension  $\mathbf{f}$  is calculated and distributed into the fixed grid;
4. In the first iteration, reference pressure is estimated. After that, its value is corrected according to the mass flux residual.
5.  $\mathbf{V}^{n+1}$  is estimated via Newton iterations, using a numerical relaxation schedule, and used to calculate the mass flux  $m$  crossing the interface. The interface mass flux is distributed in the fixed grid;
6. According to boundary conditions,  $\mathbf{w}$ ,  $\mathbf{u}$  e  $P$  are obtained from Eqs. (2) and (5);
7. Density found in step 2 and flux  $\mathbf{w}$  are interpolated via distribution function in order to find the mass flux  $w_f$  and density  $\rho_f$  at the interface;
8. Heat flux  $q$  is calculated through Eq. (9) and distributed into the fixed grid;
9. According to boundary conditions, energy equation - Eq. (7) is used to obtain the temperature at time  $n+1$ ;
10. Temperature and pressure are interpolated to find  $T_f$  and  $P_f$  at the interface;
11. The equilibrium condition is tested. If it is not satisfied, a new estimate for  $\mathbf{V}^{n+1}$  is calculated and returns to step 5.
12. The mass flux residual is calculated, and if it is lower than the reached tolerance, the fields of viscosity and conductivity are updated for the new position, advance one step time, otherwise returns to step 4.

The convergence criterion used in step 11 is the residual in Eq. (11). Once it has reached the desired tolerance, convergence for interface velocity is assumed. Otherwise, the velocity is corrected via Newton Iterations, given as:

$$\mathbf{V}^{n+1} = \mathbf{V}^n - \omega \cdot R(T) \quad (18)$$

where  $\omega$  is a constant and  $R(T)$  is the residual for the temperature jump condition at the interface. Iteration are repeated until  $R(T)$  in every point become smaller than the tolerance. The optimum value for  $\omega$  is found by tentative, at the beginning of the calculation.

A similar schedule is used to obtain the reference pressure, where the mass flux residual is the algebraic summation of the source term  $M$ , Eq. (3), along the interface.

## 4. Results

FORTTRAN language was used to construct the numerical code and it may be ran in a PC 800 MHz microcomputer. The transport equations were solved in a regular displaced mesh, via finite volume method, where the P-V coupling schedule used was the PRIME algorithm, and the discretization was done under the FTCS schedule.

### 4.1. Validation of the numerical method

The numerical results were validated by a variation of the one-dimensional Stefan problem, within a  $0 < x < 1$  domain, with a constant heat flux at  $x = 0$ , and constant temperature at  $x = 1$ . The initial interface position is  $x_f = 0.5$ , with the liquid phase at  $x < 0.5$  and vapor phase at  $x > 0.5$ . Both phases are at saturation temperature when a heat flux  $q$

is imposed at  $x = 0$ . The values used were  $K_v/K_l = 0.33$ ,  $\rho_v/\rho_l = 0.5$ ,  $c_v/c_l = 0.5$ ,  $q = 0.1$ ,  $T_{sat} = 1$ ,  $Pe = 0.04$ ,  $Re = 0.08$  and  $We = 0$ .

The results for the interface velocity are compared to those obtained via the Generalized Integral Transform Technique - GITT (Cotta et al, 1998). In Fig. (4), good agreement between both methods of solution is observed. The numerical solution improves as the number of points of Lagrangian mesh ( $n_i$ ) increases. This improvement is remarkable at the initial and steady state times. In this case, the number of points of the Eulerian mesh also increases, due the meshes coupling by the Distribution Function.

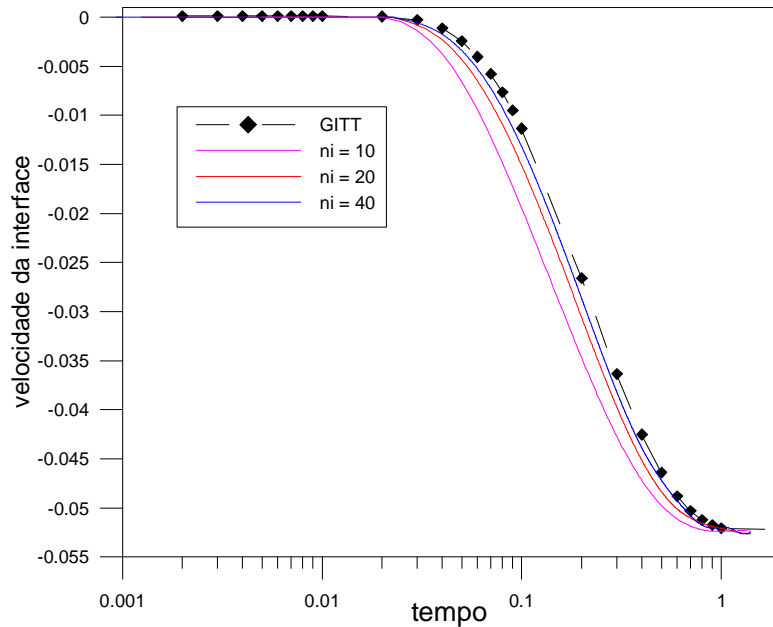


Figure 4. Comparison between Interface Tracking Method and GITT.

In Fig. (5) the effect of the interface thickness may be observed in the profiles of pressure and vertical velocity component. The thickness reduces as the number of points used increases. With  $n_i = 10$ , interface thickness occupies a considerable fraction of the domain. With  $n_i = 40$ , the discontinuity at the interface is represented with a good precision. When few points are used in the Lagrangian mesh, the results out of the interface are very close to the exact values, that are reached when  $n_i = 20$ .

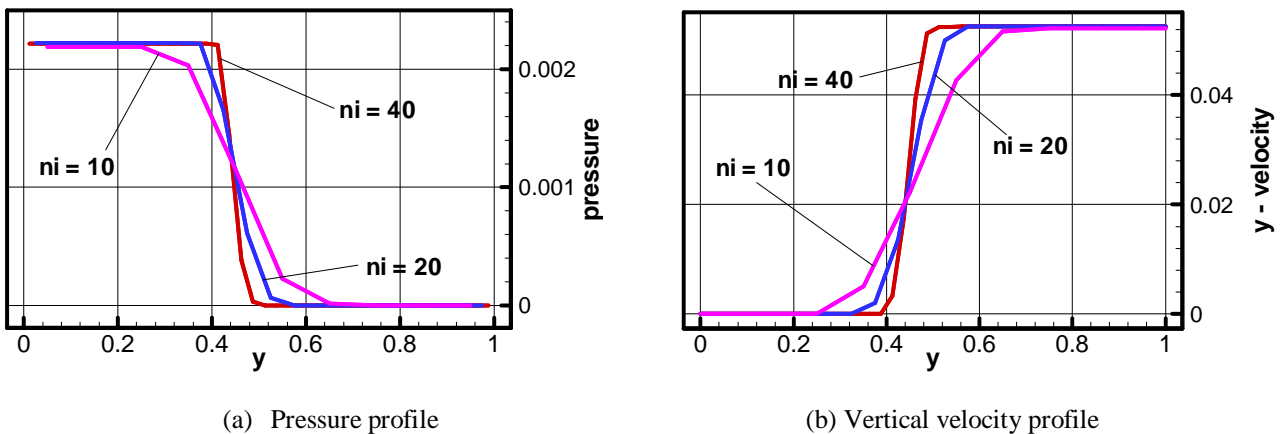


Figure 5. Solutions according the number of points used in the Lagrangean mesh ( $n_i$ ).

#### 4.2. Results for a square cavity

Preliminary results for 2-D unsteady simulation were obtained for a flat square cavity representing a capillary heat pipe, considering the effects of gravity and surface tension. The domain considered is the region defined as  $0 < x < 1$  and  $0 < y < 1$ , under a wall heat flux of  $q_w = 0.1$ , in  $0 < x < 0.5$ , and  $q_w = -0.1$  in  $x > 0.5$ . The lateral and superior walls are insulated. The values used in the test case, for the physical parameters, were:  $K_v/K_l = 1$ ,  $\rho_v/\rho_l = 0.9$ ,  $c_v/c_l = 1$ ,  $Pe =$

1,  $Re = 1$ ,  $We = 1$ ,  $Fr = 1$ ,  $\sigma = 0.002$  e  $\vartheta = 0.002$ , and the interface is placed at  $y = 0.5$  at  $t = 0$ . A  $20 \times 20$  points grid was used.

The schedule for correct the reference pressure was tested using an simplified second order polynomial as the equation of state:

$$T_{SAT} = 0.01.(P + P_{\infty})^2 + T_{v0} \quad (19)$$

where  $T_{v0}$  is the saturation temperature for the initial reference pressure, equal to 1. For this case, the initial value for the reference pressure is taken to zero.

Convergence of the reference pressure is shown in Fig. (6). The final value, reached in the steady state condition, seems to oscillate around the correct one. A more refined grid should be tested, so as to confirm such behavior. The curve becomes more stable as the number of grid points rises.

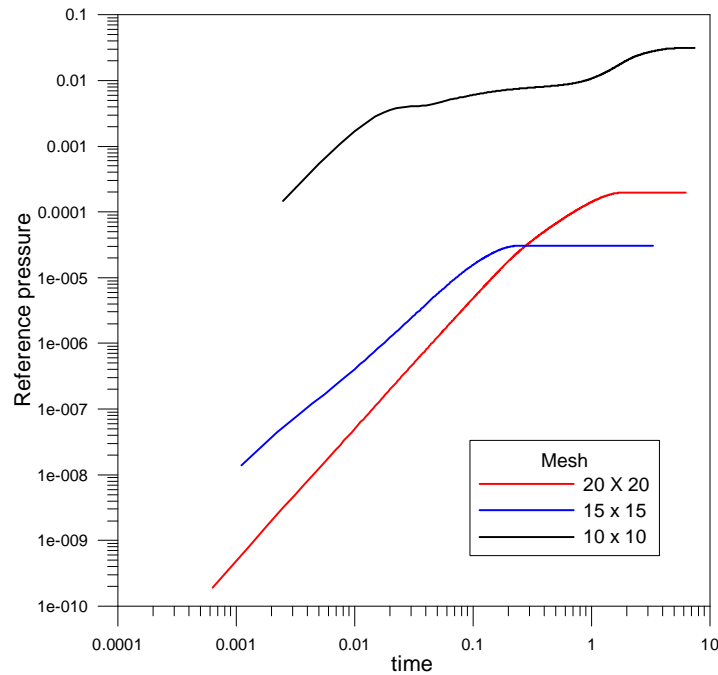


Figure 6. Convergence of reference pressure according to the grid refinement.

In Fig. (7), the evolution of interface position with the time (starting as an horizontal line) is shown, demonstrating the good behavior of the grid reconstruction schedule. At  $t = 1$ , the interface displacement is still small, although it indicates the tendency for its final profile. Steady state profile is shown at  $t = 5$ .

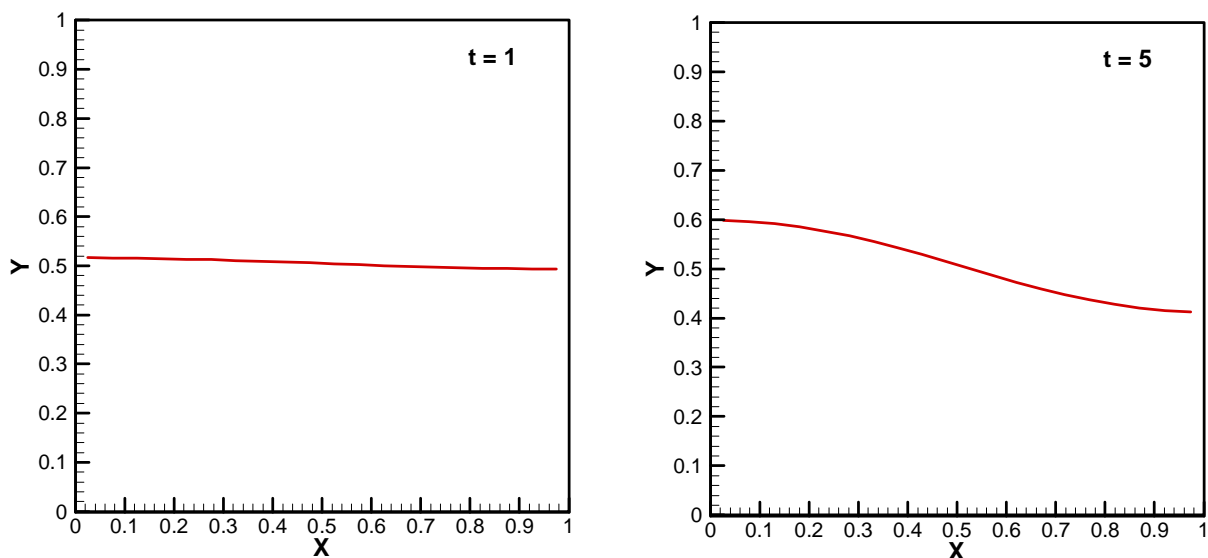


Figure 7. Evolution of interface along the time.

At the steady state, the interface concavity is clearly inverted after half-length in the x direction, that is the point that separates the condenser and evaporator sections. A similar inversion occurs in the pressure jump at the interface, caused by the effect of the interface curvature over the interfacial tension, Fig (8.a). Temperature variation occurs only in the liquid phase, Fig. (8.b), while vapor phase remains at the saturation temperature. In both cases, the blue region corresponds to the liquid phase and the red region to the vapor phase.

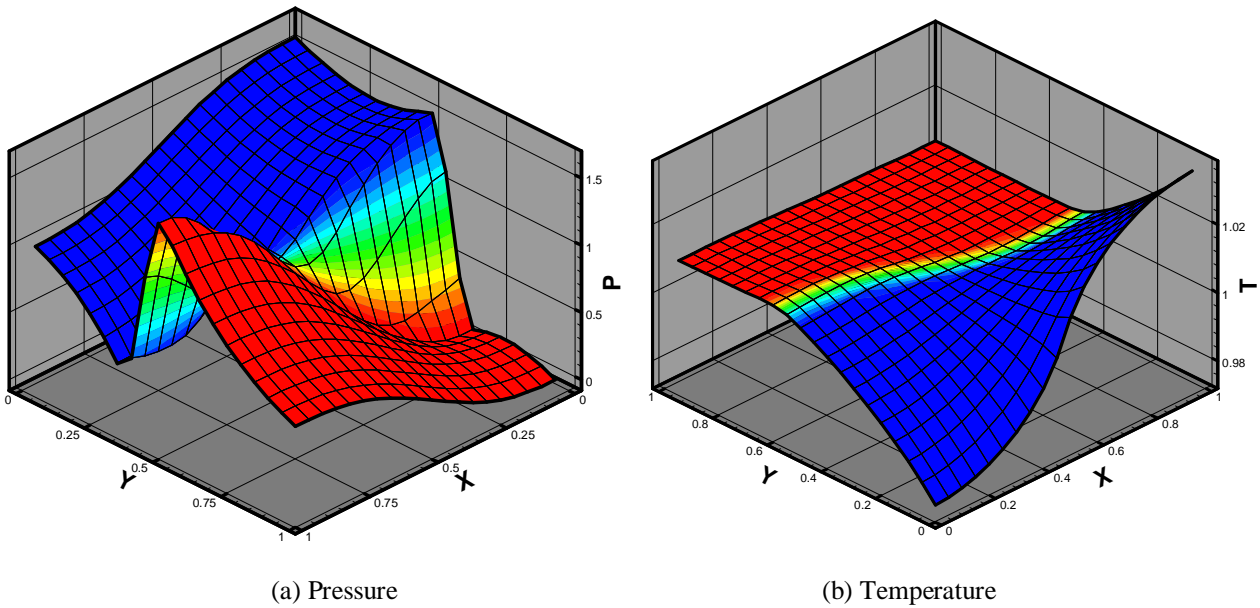


Figure 8. Pressure and temperature fields in steady state ( $t = 5$ ).

Figure (9) shows the streamlines for the steady state. The fluid circulates around the center of the interface (the red line), which is placed exactly between the condenser and evaporator region, as expected for a heat pipe, and yields the high thermal conductance of this kind of system.

Figure (10) shows the temperature and pressure variation in the interface, at  $t = 5$ . The temperature profile oscillates due the variation of the radius and center of curvature. The variation of pressure is mainly influenced by the increase of the hydrostatic pressure.

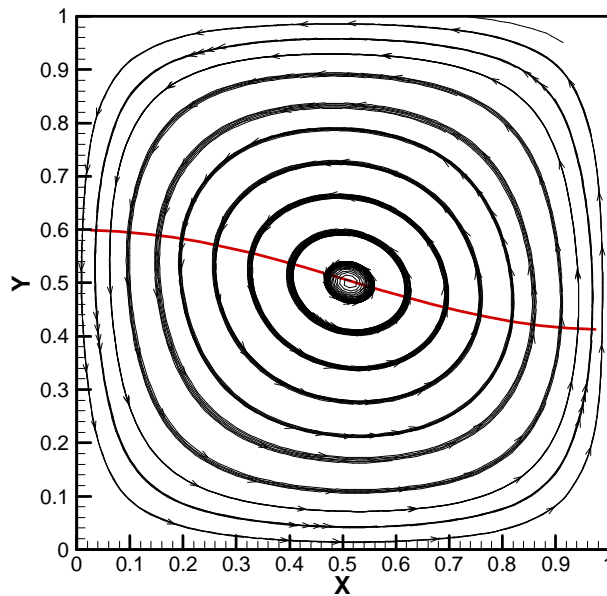


Figure 9. Stream lines at  $t = 5$  (steady state).

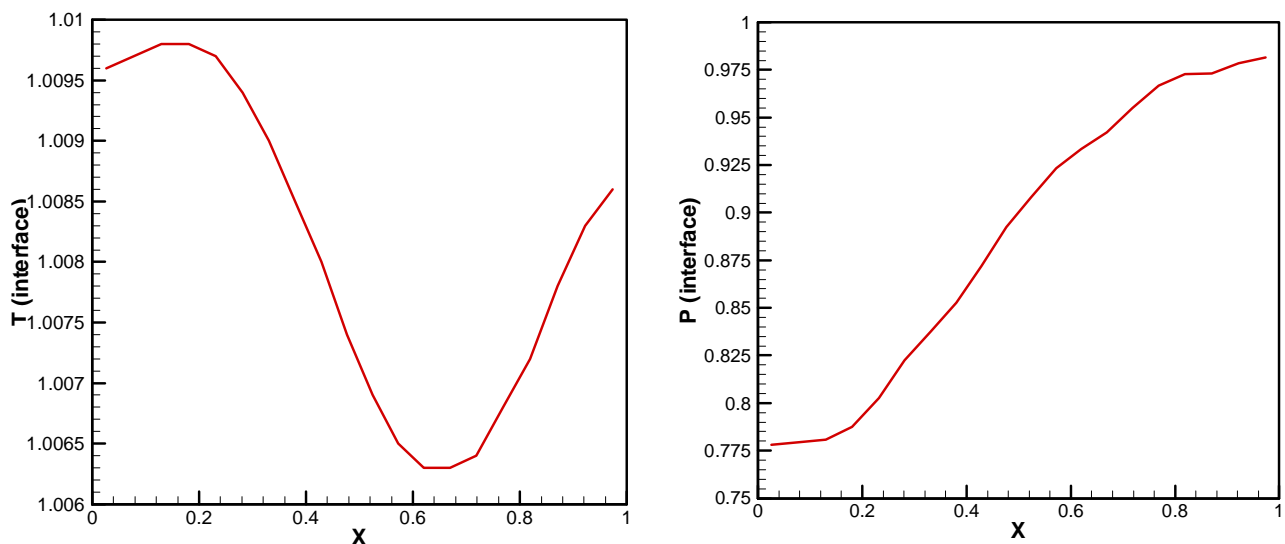


Figure 10. Pressure and temperature profiles along the interface at  $t = 5$  (steady state).

## 5. Conclusion

In this work, the Interface Tracking Method was employed to simulate the unsteady 2-D heat transfer process inside a flat capillary heat pipe, represented by a square closed cavity. The code was validated comparing its results to an exact solution of an one-dimensional problem, demonstrating its capacity to represent the interface discontinuity. Such representation improves as more points are added to the Lagrangean mesh.

The complete physical model was tested, and the method shown to be able to capture the pressure jump across the interface. The convergence for the reference pressure was analyzed, showing an oscillating convergence forward to the correct value, what have to be confirmed with the use of more refined meshes. The results present physical coherence and are qualitative close to that expected for a heat pipe. Complete test for fluids and dimensions found in feasible heat pipes are necessary for comparison to the one-dimensional models available in literature, in order to verify the accuracy of the physical model. The methodology described in this work can be extended easily to three dimensions and irregular geometries.

## 6. Acknowledgements

The author would like to acknowledge to FAPESP - the scientific sponsor agency of the Brazilian State of São Paulo - for the financial support during this work.

## 7. References

- Cotta, R. M., 1998, *The Integral Transform Method in Thermal and Fluids Science and Engineering*, Begell House, New York.
- Duncan, A. B., Peterson, G. P., 1994, Review of Microscale Heat Transfer, *Applied Mechanics Review*, v. 47, n. 9, pp. 397-428.
- Faghri, A., 1995, *Heat Pipe Science and Technology*, Taylor&Francis, NY.
- Juric, D., 1996, *Computations of Phase Change*, PhD. Thesis, University of Michigan.
- Juric, D. and Tryggvason, G., 1998, Computations of Boiling flows, *Int. J. of Multiphase flow*, vol. 24, no. 3, pp 387-410.
- Khrushstalev, D., Faghri, A., 1994, Thermal Analysis of a Micro Heat Pipe, *Journal of Heat Transfer*, Vol 116, pp. 189-198.
- Ma, H. B., Peterson, G. P., 1998, The Minimum Meniscus Radius and Capillary Heat Transport Limit in Micro Heat Pipes, *Journal Heat Transfer*, v. 120, pp. 227-233.
- Machado, H. A., Miranda, R. F., 2001, Simulation of Micro Heat Pipes Using an Interface Tracking Method, *Proceedings of the XVI COBEM - Brazilian Congress of Mechanical Engineering*, Uberlândia, Brazil.
- Peterson, G. P., 1994, "An Introduction to Heat Pipes – Modeling, Testing and Applications", John Wiley & Sons, New York..
- Peterson, G. P., Ha, J. M., 1998, Capillary Performance of Evaporating Flow in Micro Grooves: An Approximate analytical Approach and Experimental Investigation, *Journal Heat Transfer*, v. 120, pp. 743-751.
- Peterson, G. P., Ma, H. B., 1999, Temperature Response of Heat Transport in a Micro Heat Pipe, *Journal Heat Transfer*, v. 121, pp. 438-445.
- Prat, D. M., Brown, J. R., Hallinan, K. P., 1998, Thermocapillary Effects on the Stability of a Heated, Curved Meniscus, *Journal Heat Transfer*, v. 120, pp. 220-226.

- Ravigururajan, T. S., 1998, Impact of Channel Geometry on Two-Phase Flow Heat Transfer Characteristics of Refrigerants in Microchannel Heat Exchangers, *Journal Heat Transfer*, v. 120, pp. 485-491.
- Unverdi, S. O., Tryggvason, G., 1992, A Front-Tracking Method for Viscous, Incompressible, Multi-fluid Flows, *Journal of Computational Physics*, vol. 100, pp. 25-37.